2012

Measurement and Visualization of R410A Distribution in the Vertical Header of the Microchannel Heat Exchanger

Yang Zou
yangzou1@illinois.edu

Predrag S. Hrnjak

Measurement and Visualization of R410A Distribution in the Vertical Header of the Microchannel Heat Exchanger

Yang ZOU, Pega HRNJAK*

University of Illinois at Urbana-Champaign, Department of Mechanical Science and Engineering, Urbana, IL, USA
Contact Information (E-mail: yangzou1@illinois.edu, pega@illinois.edu)

* Corresponding Author

ABSTRACT

This paper presents the refrigerant adiabatic upward flow in the vertical header of microchannel heat exchanger and its effect on distribution. R410A is circulated into the header through the microchannel tubes (5 or 10 tubes) in the bottom pass and exits through tubes (5 or 10 tubes) in the top pass representing flow in the heat pump mode of reversible systems. Three circular headers were explored, each with the microchannel tubes inserted to half depth. The quality was typically varied from 0.2 to 0.8. Mass flow rate was from 1.5 to 4.5 kg/h per microchannel. The best distribution is found at high flow rate and low quality.

Distribution is improved by doubling the number of microchannel tubes although elongation of the header has negative effect. Visualization reveals the effects of flow patterns in terms of homogeneity and liquid momentum. Refrigerant in the churn flow has better distribution than in the separated flow since the two-phase mixture is more homogeneous. The distribution is better at high mass flux in the header because the higher momentum liquid can be supplied to the top exit tubes.

1. INTRODUCTION

Microchannel heat exchangers have come to the frontier of stationary air conditioning and refrigeration application after its success in mobile air conditioning systems, for their advantages in compactness and higher air-side heat transfer coefficient. In the reversible systems, microchannel heat exchanger functions as both evaporator and condenser. The outdoor heat exchanger, typically a multipass microchannel heat exchanger, has vertical header to reduce cost and for easier bending when U shape condenser is needed. The outdoor heat exchanger functions as condenser in the cooling mode and the overall flow is downward. In the heating mode, it functions as evaporator and refrigerant flows in the reversed direction. Then, refrigerant maldistribution due to two-phase flow in the vertical header deteriorates the heat exchanger's performance, and consequently reduces system efficiency. Good design that provides reasonable distribution in heat pump mode is still a challenge.

Several researchers have reported the distribution problems, mostly related to horizontal header with vertical tubes. Hrnjak (2004) and Webb and Chung (2005) have reviewed the distribution problems. Combined with others' results, it can be conceived that maldistribution is a very complex problem that is affected by numerous parameters: header geometry and orientation, fluid properties, inlet mass flux and quality, etc. In their studies of horizontal header, Fei and Hrnjak (2004), Vist and Pettersen (2004), Bowers et al. (2006) and Hwang et al. (2007) showed that the flow pattern in the inlet tube affected the flow regimes in the header. Such flow regimes had a strong influence on liquid distribution in the two-phase flow. In the studies of vertical header, Watanabe et al. (1995) investigated the distribution of R11 in a vertical header with five round branch tubes. Along the flow direction in the header, the flow pattern transited from annular to slug or froth flow. Song et al. (2002) manifested maldistribution of CO_2 in the outdoor microchannel coil in heating mode through frosting patterns. They related distribution in the header with the balance between inertial, gravitational and shear forces. Some work of Cho and Cho (2004) was devoted to distribution of R22 in the vertical header with microchannel tubes. It was found that most liquid were in the bottom

because of gravity regardless of the inlet types. The visualization of air and water upward flow in the vertical header from Lee (2009) showed that three regions were formed. The flow patterns in these three regions were different. They had great impact on the distribution. Byun and Kim (2011) tested and visualized the distribution of R410A in both the inlet and second pass headers at one quality condition. For the inlet header, a pool was formed at the bottom. For the second pass header, a liquid film is formed in the header due to two-phase jet inlet.

It is noteworthy that the most of the tests were done in low qualities, i.e. $x_{in} < 0.5$, because the inlet header was usually studied. However, typical microchannel outdoor heat exchanger has at least two passes. Two-phase refrigerant is redistributed in the intermediate header in which case distribution phenomenon is more complex but important. Thus, in this paper, refrigerant distribution in an intermediate header for a multipass heat exchanger (with capacity of 0.5-2.5 kW) was studied. The refrigerant to the header was provided by multi-parallel microchannel tubes from the inlet header.

2. EXPERIMENTAL METHOD

The test loop was constructed to model R410A distribution in the microchannel heat exchanger, as shown Figure 1. The liquid refrigerant was pumped into the inlet header while the inlet mass flow rate m_{in} was measured by mass flow meter (Micromotion D40, ±0.75%). The pump speed was controlled by a bypass valve and VFD. The temperature T_{sub} (immersed thermocouple, ±0.5 ^{o}C) and pressure P_{sub} (Sensotec TJE, ±1% FS) at the inlet to the first header were measured to determine the subcooling. The subcooled liquid was assumed to distribute evenly into microchannel tubes in the bottom pass, where the refrigerant was heated to the desired quality while the heaters are insulated. Set of six heaters per microchannel tube were providing uniformly of heat supply. The power needed to determine inlet quality was measured by watt transducer (Ohio Semitronics GW5-024CX5, ±0.2% FS). After the refrigerant entered into the lower part of the header, it turned 90^{o}, flowed upward and reached the upper part of the header. Due to maldistribution, different liquid amount exited through the microchannel tubes in the top pass. In these tubes, the refrigerant was heated again to provide equal superheat at the exit. Each tube was heated by six heaters and insulated. Each set of six heaters was individually controlled to provide adequate power to generate equal superheat, and was also measured by watt transducer (Ohio Semitronics GW5-024CX5, ±0.2% FS) separately to determine inlet quality into each exit tube. The temperature $T_{sup,i}$ (immersed thermocouple, ±0.5 ^{o}C) in each tube and pressure P_{sup} (Sensotec TJE, ±1% FS) were measured to determine the superheating. The mass flow rate of single phase superheated vapor was measured individually as the total mass flow rate for each microchannel tube by mass flow meter (Micromotion D06, ±0.15%). The vapor was then brought to the condenser. With the help of the receiver and subcooler, the subcooled liquid was provided to the pump.

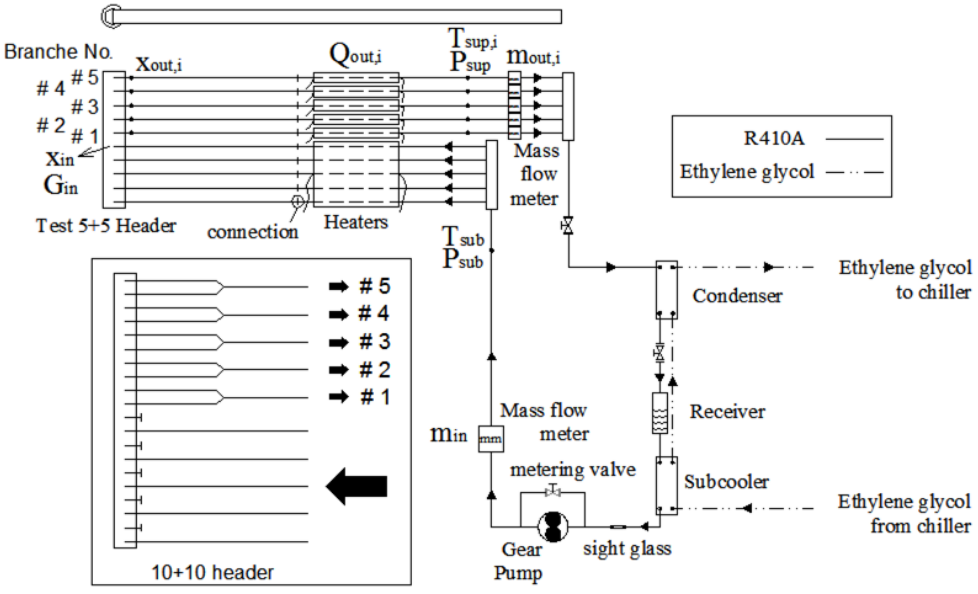

Figure 1: System schematics

Enthalpy at the superheated point $i_{sup,i}$ was determined by $T_{sup,i}$ and P_{sup}. The outlet enthalpy from the header or inlet to each exit tube $i_{out,i}$ was then calculated as

$$i_{out,i} = i_{\sup,i} - \frac{\dot{Q}_{out,i}}{\dot{m}_{out,i}} \tag{1}$$

The pressure in the header P_{ave} is estimated as the average of subcooled and superheating pressures. The outlet quality from the header $x_{out,i}$ can be found from $i_{out,i}$ and P_{ave}. Then, the liquid mass flow rate in each tube can be obtained as

$$\dot{m}_{l,out,i} = \dot{m}_{out,i}(1 - x_{out,i}) \tag{2}$$

A high speed camera, Phantom v4.2, is used for visualizing the flow patterns in the transparent header. The exposure time of the camera was set from 80 μsec to 100 μsec. The framing rate was at 2200 frames per second. The resolution was set as 512x512 or 256x512 pixels.

Three circular headers were examined, each with the microchannels inserted to half depth: 1) the aluminum header with five inlet and five exit microchannel tubes as used in industry (5+5 aluminum header), 2) the transparent replica of the first (5+5 transparent header), and 3) transparent header with ten inlet and ten exit microchannel tubes (10+10 transparent header) to study the effect of increasing microchannel number and header length. The transparent ones were made of PVC tube. The gap between microchannel tube and PVC tube was sealed by special epoxy (JB-WELD). It is the black material on the right part of the header in the images. In addition, an epoxy block was made to increase the pressure tolerance while still ensure the transparency outside the PVC tube. The inner diameter of the aluminum header is 14.94 mm, and that of the transparent header is 15.44 mm. The tube pitch is 13 mm. The 5+5 header is 170 mm long, and the 10+10 header is 300mm long. Each microchannel tube has 17 rectangular channels. The hydraulic diameter of the microchannel is calculated based on the manufacturer data to be 0.5 mm.

To examine the case of ten inlet and ten exit tubes using the same header diameter (different circuiting), modification of the facility was made with intention to maintain the same number of mass flow meters (five) and the same heaters and control strategy. Decision is made to combine two neighboring exit tubes in one with a "Y" connection, assuming that will affect resolution of the distribution parameters only, not the essence of the results. The refrigerant from the neighboring two branches was heated together to be superheated. Therefore, only five liquid flow rate results were obtained, whereas actually each one represented the liquid amount in the neighboring two branches. As shown in Figure 1, in order to facilitate the connection of the 10+10 header, only five inlet microchannel tubes were connected and allowed refrigerant to pass through implicitly assuming insignificant effect of inlet difference. The other five inlet microchannel tubes were blocked and just served as obstruction in the header.

The average saturation temperature was about 5 ^{o}C. The inlet quality was from 0.2 to 0.8. The results of x_{in} = 0 and 1 were taken to provide two asymptotes, and those of x_{in} = 0.95 were to offer more typical situation at high quality. The mass flow rate was from 1.5 to 4.5 kg/h for each microchannel. Thus, the mass flow rate in the middle of the header was from 2.14 to 6.25 g/s for 5+5 header and 4.28 to 12.50 g/s for 10+10 header, while the mass flux in the header from 11.43 to 33.38 kg/m^2-s for 5+5 headers and 22.86 to 66.76 kg/m^2-s for 10+10 header. Tests at 7.27 g/s (38.82 kg/m^2-s) for 5+5 header were taken in attempt to reach uniform distribution. Tests at 2.22 g/s (11.86 kg/m^2-s) for 10+10 header were taken to compare the results with those of 5+5 header. Based on Bowers et al. (2006), the mass flux defined by the smallest cross sectional area in the header is more representative when the protrusion is present, so the maximum mass flux in the header, G_{in}, as shown in Figure 1, will be used in the following analysis. And it was from 21.80 to 63.67 kg/m^2-s for 5+5 headers and from 22.62 to 127.3 kg/m^2-s for 10+10 header.

Two metrics are used to evaluate the distribution. The first one is coefficient of variation σ. It is the dimensionless standard deviation, which is defined as

$$\sigma = \frac{1}{\overline{m}_l}\sqrt{\frac{1}{n}\sum_{1}^{n}(\dot{m}_{l,out,i} - \overline{m}_l)^2} \tag{3}$$

Uniform distribution is described by σ = 0. The worst distribution, for this case (five results), is σ = 2. The advantage of this metrics is that one number characterizes goodness of distribution. However, in order to illustrate the distribution profile, it is necessary to apply the liquid fraction,

$$LF_i = \frac{\dot{m}_{l,out,i}}{\sum_i^n \dot{m}_{l,out,i}} \tag{4}$$

For the case of five results, uniform distribution is described by LF_i = 0.2 in every tube. The uncertainty of measuring σ is within 4.5%. The absolute uncertainty of liquid fraction is from 0.00017 to 0.015.

3. RESULTS AND DISCUSSION

3.1 Liquid fraction and coefficient of variation

Figure 2 to Figure 4 show the distribution profiles and the coefficient of variation of 5+5 aluminum (Figure 2) and transparent (Figure 3) headers and 10+10 transparent header (Figure 4). The darkness of the bar color represents different branches (tubes), the pale being lowest exit branch and the dark being highest exit branch. The best distribution indicated by σ is at x_{in} = 0.2 (the lowest) and the highest inlet mass flux among the test conditions.

The results of 5+5 aluminum and transparent headers are very similar (See Figure 2 and 3). The small discrepancy may be due to different internal areas. In Figure 2 (a) and 3, at fixed quality, the liquid fraction of the top branch is higher as mass flow rate increases and at x_{in} = 0.6, 0.8 and 0.95, the liquid fractions of the bottom branches reduce at the same time, whereas at x_{in}=0.2 and 0.4, the liquid fractions of the bottom branches do not change much. At fixed mass flow rate, the liquid fraction of the highest branch reduces as the quality increases. Meanwhile, for the other branches, as quality increases, 1) at m_{in} = 2.14 and 3.17 g/s, the bottom branches have higher and higher liquid fraction; 2) at m_{in} = 4.19 g/s, more liquid leaves at the middle tubes; 3) at m_{in} = 5.22, 6.25 and 7.27 g/s, the liquid fraction of branch 4 becomes highest while the others are less and less. Based on the values of σ in Figure 2 (b), it is seen that: 1) at fixed mass flow rate, the distribution usually deteriorates as quality increases; 2) at low qualities, the distribution improves with increasing mass flux; 3) at high qualities, the distribution is better at some intermediate mass flow rate. It gets worse as m_{in} either increases or decreases. But compared to the low quality cases, the distribution is always poor. What matters is just whether header at the higher or lower part has liquid to be entrained to branches (tubes).

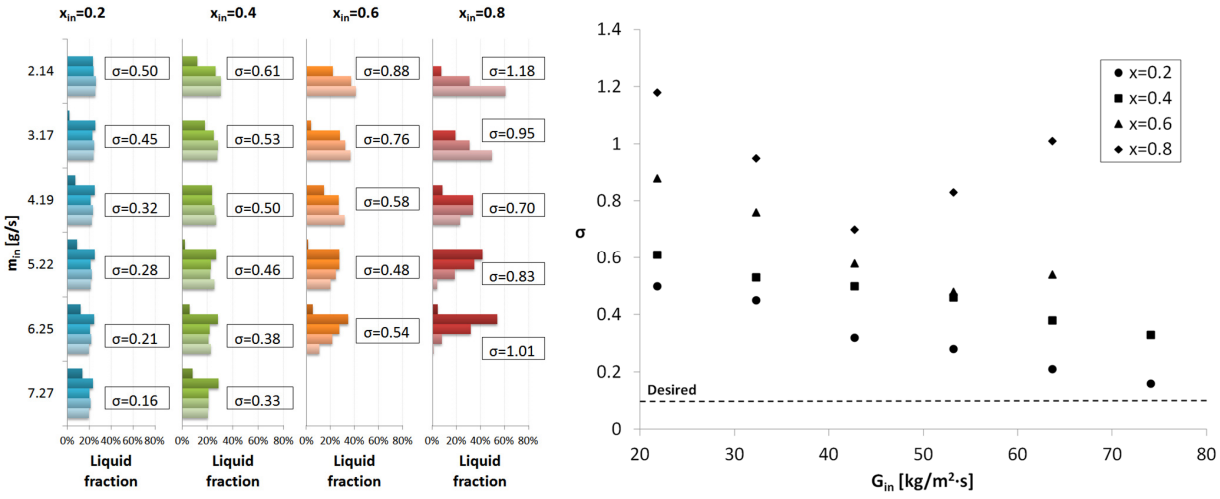

a) Liquid fraction b) Coefficient of variation

Figure 2: Distribution results of 5+5 aluminum header

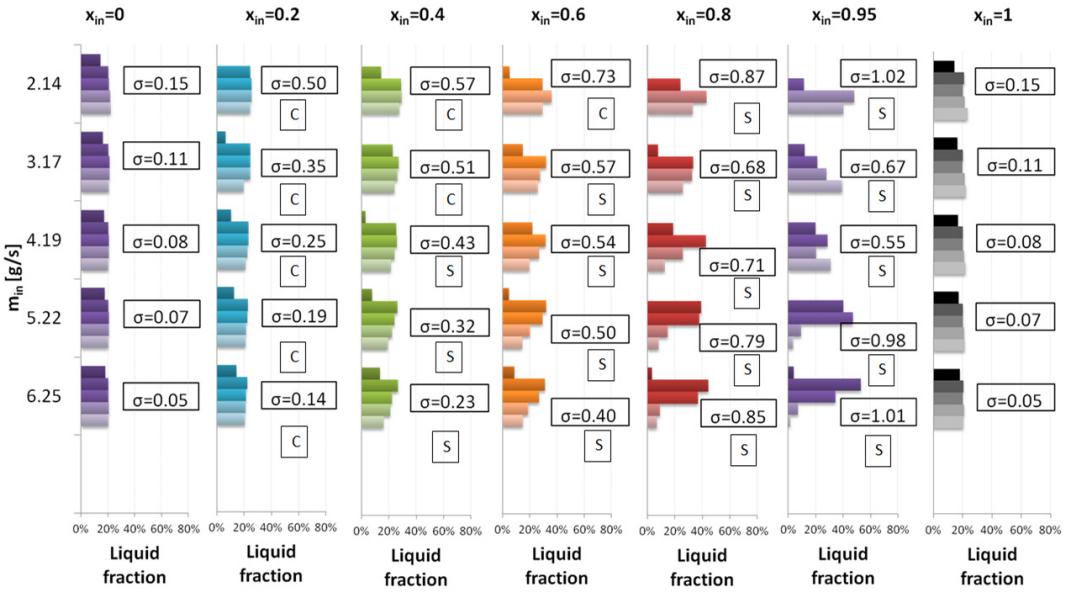

Figure 3: Distribution results of 5+5 transparent header

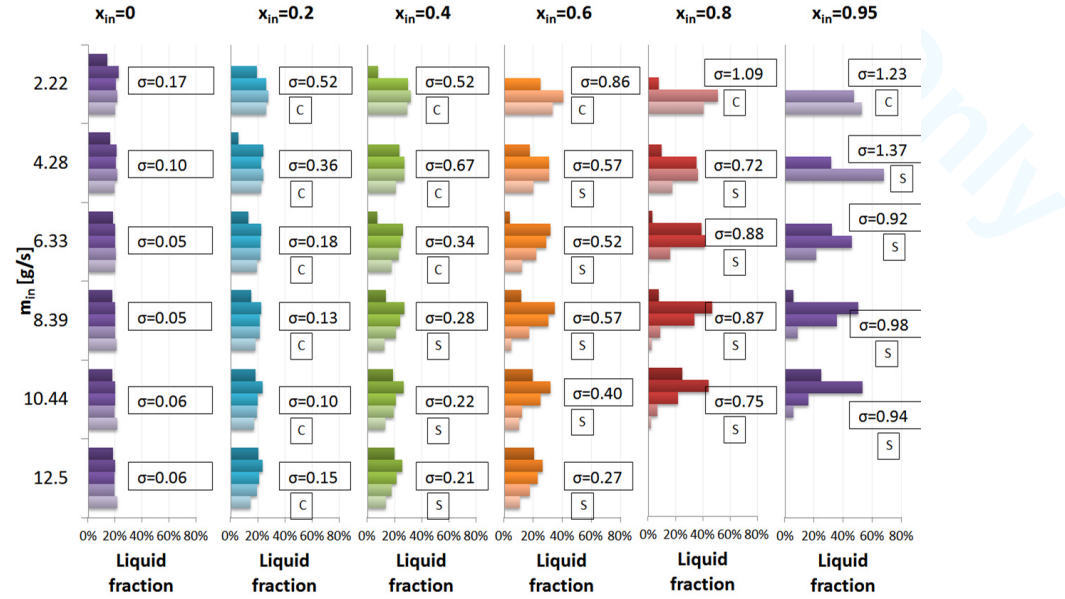

Figure 4: Distribution results of 5+5 transparent header

In Figure 4 for 10+10 header, the trend of the results is very similar as that of 5+5 header cases: for the same mass flow rate, when inlet quality increases, the distribution is worse; and for the same inlet quality, when mass flow rate increases, the distribution is improved. The mass flow rate in each inlet microchannel tube is consequence of design mostly affected by the air side heat transfer calculation. When the tube number in each pass is doubled, so is the mass flow rate in the middle of the header. This would help the top tubes to receive more liquid and hence improve the distribution. However, the header is longer than that for 5+5 configuration. It consequently requires higher inertia forces to supply the liquid to the top branch (tube). All of these factors affect the distribution profiles. However, experiment shows that distribution is usually better for the 10+10 header at the same mass flow rate in one inlet microchannel. Comparing the distribution profiles between 5+5 header (Figure 3) and 10+10 header (Figure 4) at the same mass flow rate in the header, they look very similar, so the mass flux in the header may be an important parameter in determining the distribution.

The coefficient of variation of all these distribution results can be related to liquid mass flux $G_l = G_{in}(1-x_{in})$ in the middle of the header, as shown in Figure 5. For D=15 mm, 5 or 10 inlet and 5 or 10 outlet microchannel tubes, R410A, an empirical correlation can be developed as:

$$\sigma = 9.29\times10^{-9} G_l^{\,4} - 3.29\times10^{-6} G_l^{\,3} + 4.78\times10^{-4} G_l^{\,2} - 3.35\times10^{-2} G_l + 1.07 \qquad (5)$$

This preliminary correlation can help identify possible distribution issues if σ is higher than 0.2.

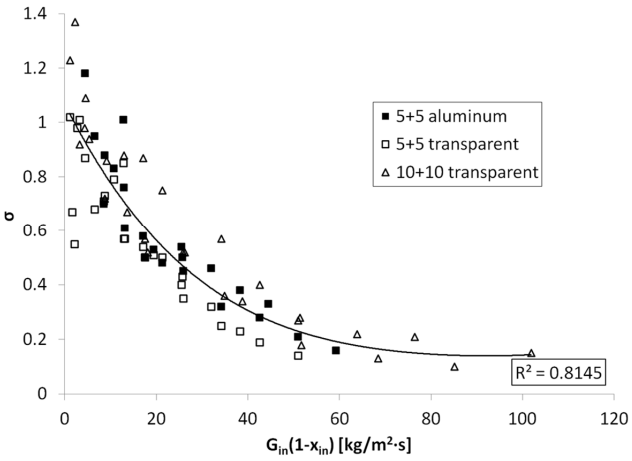

Figure 5: Empirical correlation of σ as a function of liquid mass flux

3.2 Visualization

Two flow regimes are identified from the visualization: churn and separated flow. The flow patterns are also listed in Figure 3 and 4, where "C" denotes churn flow while "S" denotes separated flow. Churn flow typically appears at low qualities, whereas separated flow usually occurs at high qualities. Increasing quality at the same mass flow rate will change churn to separated flow because of higher velocities and less liquid. Such transition is also found sometimes when increasing the mass flow rate at the same quality, e.g. x_{in} = 0.4 for 5+5 transparent header.

In churn flow, shown in Figure 6 (a), most of the header is liquid refrigerant with bubbles, but at the top it is almost vapor only. Because the horizontal velocity is small, when two-phase refrigerant enters into the header, bubbles turn and flow vertically immediately due to buoyancy effects. Liquid falls, forming a liquid pool or interacting with upward flowing vapor. Bubbles stir the liquid and form a local recirculation, although the mean velocity of liquid is upward. It is hard to distinguish the vapor and liquid interface; they are mixed almost homogenously.

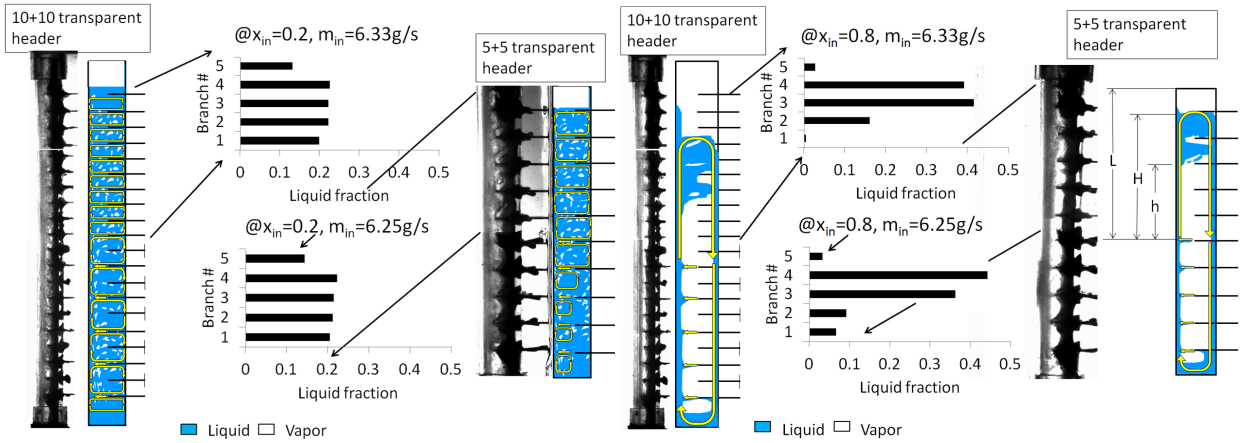

a) Churn flow b) Separated flow

Figure 6: Flow patterns in the header

However, Figure 6 (b) shows that in separated flow, the void fraction in the header is very high, and thus most the volume of the header is taken by vapor phase, but liquid is present in the form of film along the inner wall. Although the velocity from the inlet microchannel tube is high, it is still easy for vapor to turn and flow upward. However, the liquid jet at the exit from the microchannel tube flows horizontally, hits the wall and forms a liquid film. High speed vapor and the liquid film flow upward along the header. In the top exiting region, vapor phase with lighter density is much easier to turn 90^o and branch out, but liquid with larger density and higher momentum tends to run through the header and bypassed the first few microchannel tubes. The liquid film is separated from the wall at certain height. This location h, as shown in Figure 6 (b), is defined as the liquid separation height. Above the separation height, the flow pattern is locally like churn flow. Some liquid flows horizontally and leaves through the outlet microchannel tubes. Other liquid falls down through the gap between tube and round header, so that creates recirculation in the header. Finally, due to the low momentum, liquid cannot reach the top and the tubes (branches) get very little if any liquid. The highest liquid level H, as shown in Figure 6 (b), is defined as liquid reach. Above the liquid reach, there is almost vapor only. The liquid reach is also observed from churn flow in Figure 6 (a).

From Figure 6, it can be seen that the liquid distribution is better in churn flow. It is because the opportunity of liquid supply to reach each branch is increased when liquid occupies most of the header. However, in separated flow, in only a small part of the header, liquid is easily available in front of the entrance to the tube. Therefore, generalization of these two flow patterns can be used to evaluate the homogeneity of liquid and vapor phases in the header and maybe further the distribution. The generalization is accomplished by considering the two-phase flow in the header as the deviation of two-phase flow in vertical pipe. It is because: 1) flow is developing; 2) mass flux is changing along the header; 3) tubes protruding in the header obstruct the flow. Thus, the superficial momentum fluxes of liquid and vapor phases

$$\rho_l j_l^{\,2} = \frac{[G_{in}(1-x_{in})]^2}{\rho_l} \tag{6}$$

$$\rho_v j_v^{\,2} = \frac{[G_{in}x_{in}]^2}{\rho_v} \tag{7}$$

as used by Hewitt and Roberts (1969) to generalize two-phase flow in vertical pipe are applied in attempt to generalize current results. The flow regime map is shown in Figure 8 where the transition line is also identified.

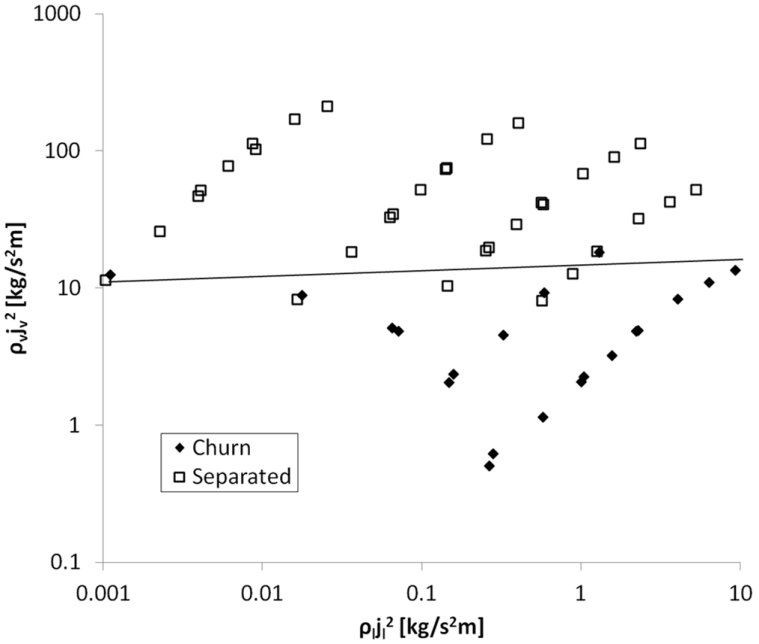

Figure 7: Flow regime map in the vertical header

However, evaluation of the homogeneity of liquid and vapor phases in the header is not sufficient to evaluate distribution. Liquid momentum is another important factor. One example is seen that at x_{in} = 0.2 from Figure 4, the top tube has no liquid at all when inlet mass flow rate is low which is because the liquid reach is below the top tube, as shown in Figure 8 (a). The liquid reach is higher when inlet mass flow rate increases, thus the distribution is better. The relative liquid reach, H/L, as defined in Figure 6 (b), is related to the liquid mass flux G_l in Figure 9. For 5+5 header, it is necessary to keep G_l above 20 kg/m^2-s, so that the liquid can reach the top tube. Such condition is G_l > 60 kg/m^2-s for 10+10 header. This is a necessary but sufficient condition for good distribution.

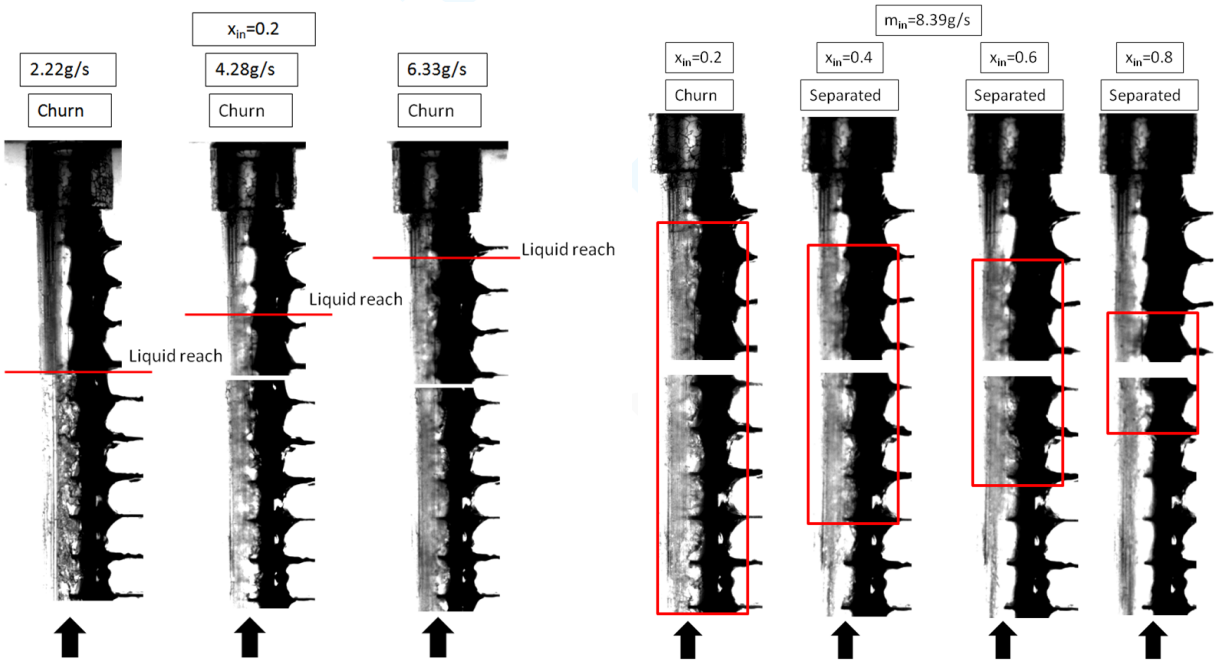

a) Liquid reach increases as flow rate increases b) Liquid separation increases as quality increases

Figure 8: Variation of liquid reach and liquid separation as flow rate and/or quality changes

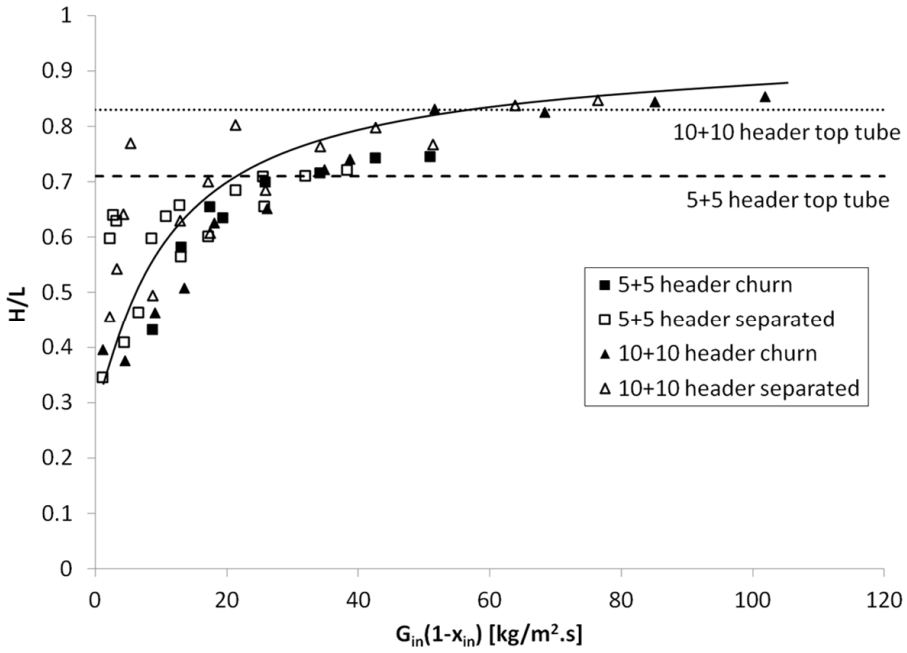

Figure 9: Generalization of relative liquid reach with liquid mass flux

As shown in Figure 8 (b), the liquid reach also changes as quality increases at the same mass flow rate. Besides, the liquid separation height in the separated flow pattern increases when the quality is higher. The relative liquid separation, h/L, as defined in Figure 6 (b), is related to gas mass flux $G_v = G_{in}x_{in}$ in Figure 10. When G_v is below 20 kg/m^2-s, the flow pattern is churn flow, and no microchannel tubes will be bypassed. This is another necessary but sufficient condition for good distribution. In order to achieve good distribution, both conditions for liquid reach and liquid separation height should be satisfied.

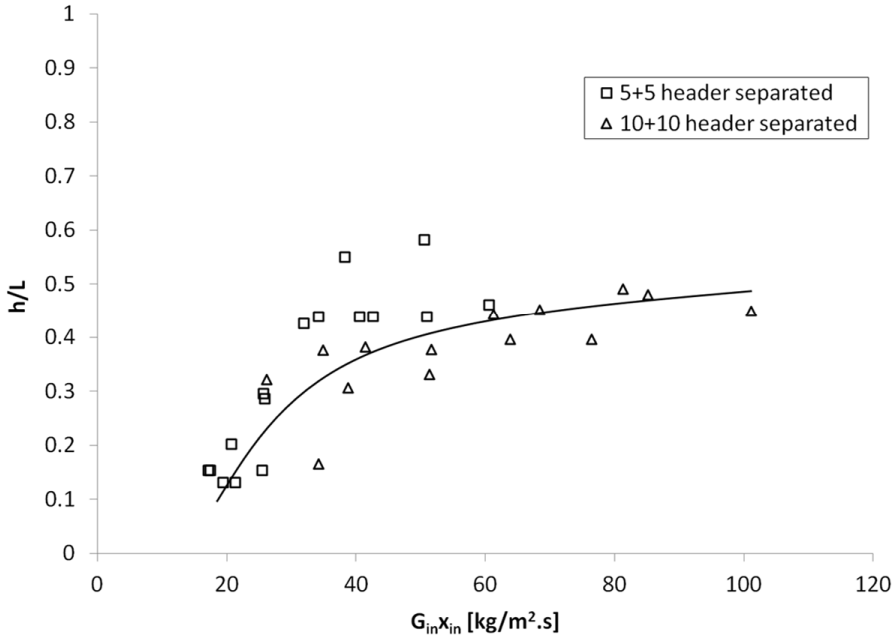

Figure 10: Generalization of relative liquid separation with vapor mass flux

4. CONCLUSIONS

The conclusions of this study are summarized below:

1) The good distribution was found at high inlet mass flow rate and low quality among the test conditions. The distribution is worse as the quality increases at the same mass flow rate. At fixed low qualities (e.g. $x_{in} \leq 0.6$), the distribution usually improves as the mass flow rate is higher. At fixed high qualities (e.g. $x_{in} \geq 0.8$), there is usually a better distribution case at some intermediate mass flow rate, but generally speaking the distribution is poor.
2) Due to increase in mass flux, greater number of the microchannel tubes improves the distribution although longer header requires higher momentum for liquid to reach the top. Comparing the results of 10+10 header with those of 5+5 header, mass flux in the header is an important parameter in determining the distribution.
3) A developed correlation for coefficient of variation (σ is a function of G_l) shows good agreement with experiment. It also shows regions of good distribution.
4) Churn and separated flow in the header were identified. The flow patterns depend upon the mass flux and quality. Churn flow transited to separated flow as the inlet quality and/or mass flux increases. Distribution is related to the flow patterns in the header. Churn flow generates better distribution because vapor and liquid phases are more homogeneous. These two flow patterns can be generalized using superficial liquid and vapor momentum fluxes.
5) Based on the visualization, axial momentum is another important factor that affects the refrigerant distribution in the header. The highest liquid level, defined as liquid reach, is generalized with liquid mass flux. In order for liquid to reach the top tube, $G_l > 20$ kg/m^2-s for 5+5 header and $G_l > 60$ kg/m^2-s for 10+10 header. In the separated flow, liquid separation height is generalized with vapor mass flux. To avoid liquid bypassing the first tube, $G_v < 20$ kg/m^2-s.

NOMENCLATURE

D	Header diameter	(m)
G	Mass flux	(kg/m^2-s)
H	Liquid reach	(m)
h	Liquid separation height	(m)
i	Enthalpy	(kJ/kg)
j	Superficial velocity	(m/s)
L	Length of the header exit part	(m)
LF	Liquid fraction	(-)
m	Mass flow rate	(g/s)
n	Number of the outlet tubes	(-)
Q	Power of the heaters	(kW)
P	Pressure	(kPa)
T	Temperature	(K)
x	Quality	(-)
ρ	Density	(kg/m^3)
σ	Coefficient of variation	(-)

Subscripts

ave	Average pressure
i	Branch number
in	At the smallest area in the middle of the header
l	Liquid
out	Out of the header
sup	Superheated
sub	Subcooled
v	vapor

REFERENCES

Bowers, C.D., Hrnjak, P.S., Newell, T.A., 2006. Two-phase refrigerant distribution in a micro-channel manifold. *Proc. 11th Int. Refrigeration Air Conditioning Conf. at Purdue*, R161.

Byun, H.W., Kim, N.H., 2011. Refrigerant distribution in a parallel flow heat exchanger having vertical headers and heated horizontal tubes. *Exp. Thermal Fluid Sci.* 35, 920-930.

Cho, H., Cho, K., 2004. Mass flow rate distribution and phase separation of R-22 in multi-microchannel tubes under adiabatic condition. *Microscale Thermophysical Eng.* 8 (2), 129-139.

Fei, P., Hrnjak, P.S., 2004. Adiabatic Developing Two-Phase Refrigerant Flow in Manifolds of Heat Exchangers. *Technical Report TR-225, Air Conditioning and Refrigeration Center, Univ. Illinois at Urbana-Champaign.*

Hewitt, G.F., Roberts, D.N., 1969. Studies of two-phase flow patterns by simultaneous X-ray and flash photography. *AERE-M 2159*, HMSO.

Hrnjak, P., 2004. Flow distribution issues in parallel flow heat exchangers. ASHRAE Annu. Meet. AN-04-1-2.

Hwang, Y., Jin, D.H., Radermacher, R., 2007. Refrigerant distribution in minichannel evaporator manifolds. *HVAC&R Res.* 13 (4), 543-555.

Lee, J.K., 2009. Two-phase flow behavior inside a header connected to multiple parallel channels. *Exp. Thermal Fluid Sci.* 33, 195-202.

Song, S., Bullard, C.W., Hrnjak, P.S., 2002. Frost deposition and refrigerant distribution in microchannel heat exchangers. *ASHRAE Trans.* 108 (2), 944-953.

Vist, S., Pettersen, J., 2004. Two-phase flow distribution in compact heat exchanger manifolds. *Exp. Thermal Fluid Sci.* 28, 209-215.

Watanabe, M., Katsuta, M., Nagata, K., 1995. General characteristics of two-phase flow distribution in a multipass tube. *Heat Transfer-Japanese Res.* 24, 32-44.

Webb, R.L., Chung, K., 2005. Two-phase flow distribution to tubes of parallel flow air-cooled heat exchangers. *Heat Transfer Eng.* 26 (4), 3-18.

ACKNOWLEDGEMENT

This project was completed in 2010. It was conducted at Air Conditioning and Refrigeration Center at the University of Illinois at Urbana-Champaign, sponsored by Daikin Industries, Ltd., and also supported by Creative Thermal Solutions. The authors are grateful to Hyunyong Kim from Daikin Industries, Ltd. for his support, help and advices during execution of this project.